ISBN: 978-3-95450-248-6 ISSN: 2673-5490 doi: 10.18429/JACoW-IPAC2025-THPB042

# DESIGN AND FIRST PROTOTYPE RESULTS OF PETRA-IV PERMANENT MAGNET DIPOLES-QUADRUPOLES

M. Tischer*, M. Gehlot, T. Ramm, P. Vagin, S. Yamin, Deutsches Elektronen-Synchrotron DESY, Germany, J. Chavanne, ESRF, Grenoble, France



*Abstract*

Permanent magnet-based dipoles will be an essential part of the future PETRA-IV light source at DESY. The bending magnets are combined-function dipole-quadrupole magnets, which provide moderate focusing with a B/G ratio of about 0.03m. Each magnet consists of several C-shaped modules, one of the three types additionally having a stepwise longitudinal gradient (DLQ). Several prototype modules have recently been manufactured. The paper describes the magnet design, compares manufacturing peculiarities, and discusses first magnetic measurement results.

## INTRODUCTION

The PETRA IV project [1,2], a major upgrade of the existing PETRA III facility, will adopt a hybrid six-bend achromat (H6BA) lattice architecture that incorporates exclusively permanent magnet (PM) based bending magnets. This approach builds on recent success such as the ESRF's Extremely Brilliant Source (EBS), where permanent magnet dipoles with longitudinal field gradients have already been implemented effectively [3,4], and aligns with recent achievements like the SLS-2 upgrade, which is also making extensive use of PM magnet technology [5,6].

All bending magnets in PETRA IV will be designed as combined-function elements, providing not only the required dipole field but also a moderate quadrupole gradient. To validate this novel magnet concept, a prototype dipole–quadrupole (DLQ) magnet is currently under development. This prototype plays a critical role in demonstrating the feasibility of the proposed design by verifying that it meets stringent operational demands and magnetic field quality requirements. Comprehensive testing will include precise magnetic field mapping to assess field uniformity, stability, and accuracy, along with mechanical evaluations to ensure structural integrity under operational and environmental conditions. Additionally, the prototype will be used to optimize fabrication processes, alignment strategies, and assembly tolerances, while also addressing challenges such as end-field effects and the fine-tuning of gradients through shimming. The successful validation of the DLQ prototype will confirm the viability of implementing PM-based combined-function magnets in PETRA IV, promising enhanced performance, reduced power consumption, and lower maintenance requirements for long-term operation.

*markus.tischer@desy.de

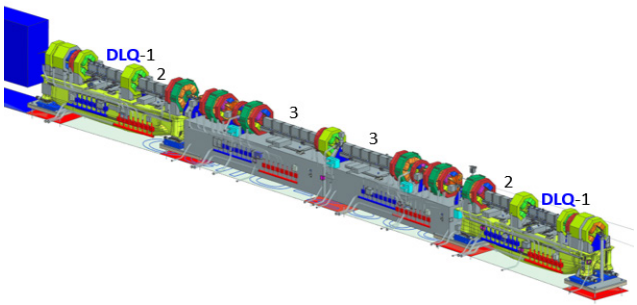


Figure 1: PETRA IV storage ring H6BA cell showing the DLQ-1,2,3 magnets.

## DESIGN CONCEPT OF DLQ

Three different types of permanent magnet dipoles are used in the H6BA cell, as illustrated in Fig. 1. Among these, the DLQ1 magnet features both transverse and longitudinal field gradients. It is composed of four modules (M4–M1) with a stepwise decrease in magnetic field of approximately 23%, while maintaining a constant field-to-gradient ratio (B/G). The other two types, DLQ2 and DLQ3, comprise only a transverse gradient. DLQ2 consists of four modules, each with identical magnetic field strength and gradient. DLQ3 includes six modules, also with uniform magnetic field and gradient across all modules. Figure 2 shows the cross-sectional view of the DLQ1 from the magnetic model and full model. Further details can be found in Refs. [7,8].

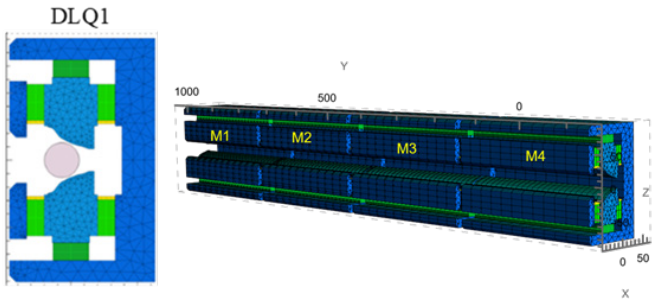


Figure 2: Magnetic model of the DLQ1 combined-function dipole.

## PROTOTYPE STATUS

The magnetic design phase has been completed for DLQ1, including comprehensive 3D simulations using Radia [9] to account for crosstalk-effects [7]. In parallel to the

ISBN: 978-3-95450-248-6 ISSN: 2673-5490 doi: 10.18429/JACoW-IPAC2025-THPB042

prototype fabrication, material studies were made for both, the SmCo permanent magnet material and also the soft-iron for poles and yoke.

Helmholtz and stretched wire measurements were done to examine several SmCo PM blocks. The measured remanence $B_r$ was about 1% lower than the specified value by the supplier (1.13T) which is still within the error bar of our assessment due to some uncertainty of the assumed susceptibility value. The $B_r$ temperature coefficient was determined by permagraph and also temperature dependent Helmholtz measurements. Both results agree within 10ppm/K and obtain a value of 390ppm/K which is ~25% higher than the 1-digit value of 0.03%/K in the data sheet.

Three different low-C soft-iron materials were processed. Materials P1 and P2 are metallurgically the same but originate from two different batches of the same supplier. The B-H measurement of the samples was done by a CERN-type permeameter. Small changes (0.2%) in the quadrupole strength were observed for the three sample materials which are well within the tuning margin. Figure 3 shows that there are also visible differences in higher harmonic components to those obtained from the usually modelled soft-iron material. This change in the sextupole component is, however, of the same order as errors expected from manufacturing or assembly tolerances, and need to be corrected in the magnetic tuning.

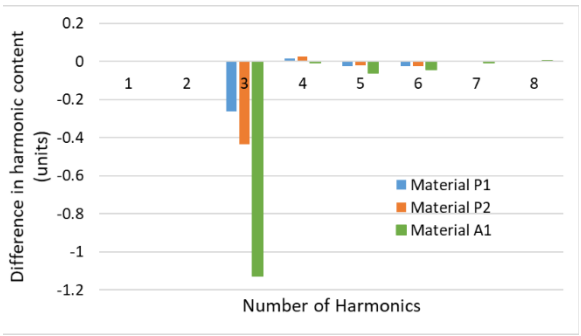


Figure 3: Change in higher harmonics of DLQ1 for simulations with B-H curves of the different characterized materials with respect to the result by the model curve.

Seven DLQ magnet modules were fabricated by three manufacturers who also followed different manufacturing strategies like standard milling or use of mold cutters. Coordinate Measuring Machine (CMM) data were collected from each manufacturer and compared to internal data from our in-house quality assurance. No significant discrepancies between the two datasets were found.

When comparing to the ideal pole profile, a small deviation in the order of 50 µm is observed across all modules. An example is given in Fig. 4. It is important to note that this deviation only reflects the shape of the pole profile. In addition to profiling, the CMM data were analyzed for mechanical misalignment errors like horizontal or vertical offsets, or angular deviations. These deficiencies will be checked for correlations with magnetic errors in the further course of magnetic measurements and tuning of the prototype modules.

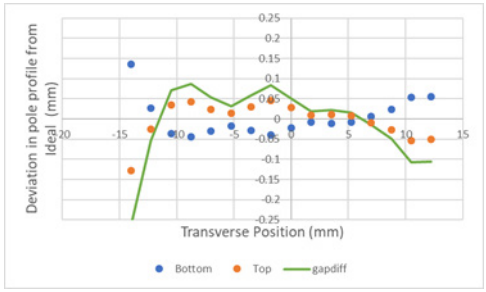


Figure 4: Deviation of CMM data from the ideal pole profile for one of the modules. The green line shows the difference in total gap.

A dedicated mechanical tooling system has been built which is based on an ESRF development to enable a precise and safe insertion of the permanent magnet blocks into the yoke. Also, one of the empty magnet modules was measured by a Hall probe to check for potential residual fields imprinted during the manufacturing process. All observed field distortions were found to be in the order of the ambient field level.

## MAGNETIC MEASUREMENTS

Magnetic field measurements and fine-tuning of individual modules, as well as the complete assembly, are conducted using a high-precision stretched-wire measurement bench acquired from the ESRF [10]. The mechanical alignment of the linear stages was performed using a FaroArm, the positional accuracy and repeatability of the wire trajectory was referenced against a laser interferometer. A first high-field prototype module is currently characterized by stretched wire measurements (Fig. 5). In this preliminary configuration of the module, end poles are mounted but iron shims are still missing as well as the correct amount of thermal shims. Figure 6 shows the related measurement of the vertical 1st field integral and the derived gradient as a function of the transverse position. Figure 7 compares the higher harmonic components obtained from a circular measurement at 8 mm reference radius with those of a Radia simulation for this module configuration; the measurement was done at a transverse position corresponding to

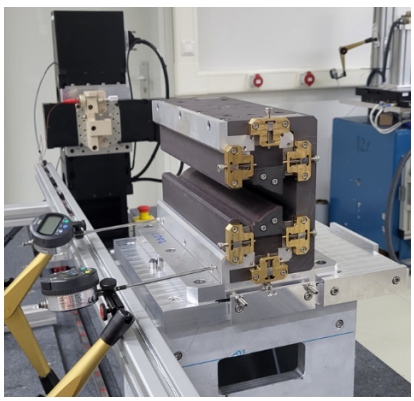

Figure 5: High-field DLQ1 module M4 at the stretched wire bench.

ISBN: 978-3-95450-248-6 ISSN: 2673-5490 doi: 10.18429/JACoW-IPAC2025-THPB042



the target value of the field-to-gradient ratio B/G. The residual higher harmonics in the simulation reflect both, the not yet complete configuration and particularly also the crosstalk to the adjacent module which is considered in the design but does not appear in this isolated single module measurement. While b4 agrees within 0.5 units, the deviation in b3 is about +2 units and needs to be corrected in the shimming process.

The magnetic signatures of thermal and iron shims have been measured and compared to simulation results. Thermal shims will be used to compensate temperature dependent effects of the permanent magnets to assure a stable field characteristic under operation conditions. Iron shims will be placed on top of the thermal shims at the magnet side rows to adjust the quadrupole strength and to correct higher order harmonics as well as spurious skew components. The signatures in Fig. 8 refer to full length (280x13mm$^2$) with 0.35 mm thickness.

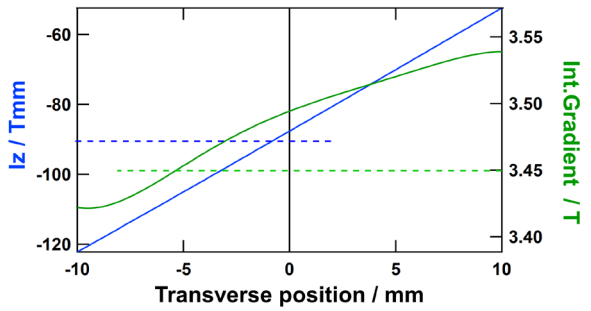


Figure 6: Initial measurement (as assembled) of vertical field integral and integrated gradient of the first DLQ1 high-field module; dashed lines indicate target values.

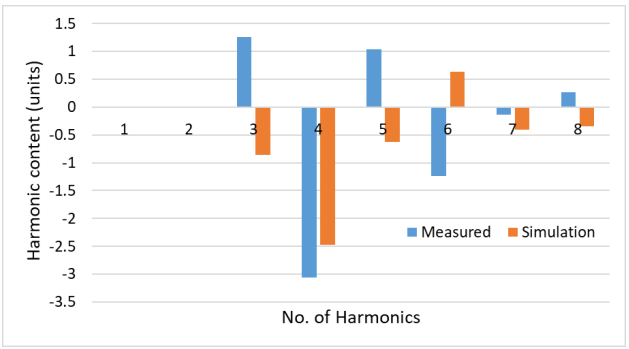


Figure 7: Comparison of measured and simulated higher harmonics of a DLQ1 high-field module (in intermediate configuration, see text); quadratic sum of simulated harmonics: $2.8\times10^{-4}$.

Obviously, vertically asymmetric placement of shims (top or bottom rows only) introduces a strong skew correction of 0.28 Tmm and 0.15 Tmm for a1 and a2, respectively, and can also be used to compensate remaining vertical position errors. On the other hand, horizontally asymmetric placement of shims (e.g. only at open or closed side of the yoke in Fig. 8.a) show a different response in the b1 vs. b2 contribution. More important, however these two configurations show an opposite signature in b3 with a difference of ~0.06 Tmm that can be exploited to mitigate normal sextupole errors. Similarly, a pronounced difference is found in the normal sextupole contribution of the shim signature of the transversely placed movable shunts at the outer ends of each DLQ. Each single DLQ module will firstly be measured and tuned individually. Subsequently, each fully assembled DLQ magnet will be tuned to meet the field quality specifications.

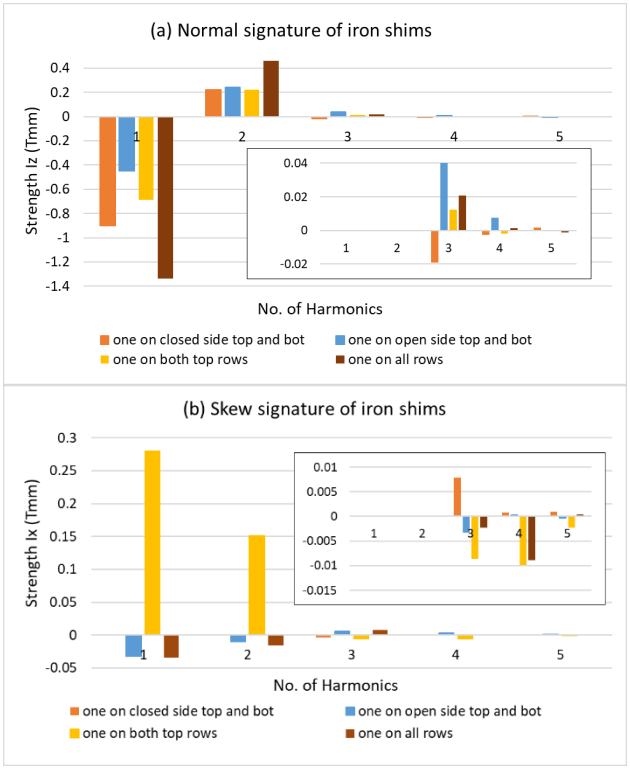


Figure 8: Normal (a) and skew (b) signatures of various iron shim configurations placed on top of the magnet side rows.

## CONCLUSION

The present design, fabrication, and initial testing of the DLQ1 prototype modules support the feasibility of using permanent magnet-based combined-function dipoles for PETRA IV. Magnetic measurements are in good agreement with simulations, and all modules meet the required mechanical tolerances. The effectiveness of the shimming techniques allows precise tuning of the field quality. The observed multipole components are within limits that are covered by the tuning margin included in the design of each of the module types.

The next phase will focus on verifying the intended shimming concept by tuning 4 modules to specification in order to integrate them to a full DLQ1 assembly which shall then be fine-tuned to comply with a cumulative harmonic error below $5 \times 10^{-4}$. Further work will include the evaluation of the thermal performance of the DLQ modules, and the development of a reliable fiducialization procedure.

ISBN: 978-3-95450-248-6 ISSN: 2673-5490 doi: 10.18429/JACoW-IPAC2025-THPB042

# REFERENCES


[1] R. Bartolini *et al*., "Status of PETRA IV Machine Project", in *Proc. IPAC2022*, Bangkok, Thailand. doi:10.18429/JACoW-IPAC2022-TUPOMS029.

[2] I. Agapov *et al*., "Magnet Design for PETRA IV Storage Ring", in *Proc. IPAC2022*, Bangkok, Thailand. doi:10.18429/JACoW-IPAC2022-THPOTK002

[3] G. Le Bec *et al*., "Magnets for the ESRF Diffraction-Limited Light Source Project," in *IEEE Transactions on Applied Superconductivity*, vol. 26, no. 4, pp. 1-8, June 2016. doi:10.1109/TASC.2015.2510402

[4] C. Benabderrahmane *et al.*, "Status of the ESRF-EBS Magnets", in *Proc. IPAC'18*, Vancouver, Canada, Apr.-May 2018, pp. 2648-2651. doi:10.18429/JACoW-IPAC2018-WEPMK009

[5] S. Sanfilippo, "Magnets for the upgrade of the Swiss light source. at the Paul Scherrer Institute-design, production, measurement challenges", *IEEE transactions on applied superconductivity*, vol 34, no. 5, August 2024. doi:10.1109/TASC.2023.3335029

[6] M. Böge, "SLS 2.0 storage ring commissioning", WECN1 contribution at IPAC 25, these proceedings.

[7] M. Gehlot, J. Chavanne, P. N'gotta, T. Ramm, and M. Tischer, "Design of permanent magnet dipoles-quadrupoles with longitudinal gradient for the PETRA IV storage ring", in *Proc. IPAC'23*, Venice, Italy, May 2023, pp. 3798-3800. doi:10.18429/JACoW-IPAC2023-WEPM100

[8] M. Gehlot *et al*, "Progress in Design of Permanent Magnet Dipole-Quadrupoles with Longitudinal Gradient for the PETRA IV Storage Ring", in proceedings of SRI 2024 in J. Phys.: Conf. Ser. 3010 (2025).

[9] P. Elleaume, O. Chubar and J. Chavanne, "Computing 3D magnetic fields from insertion devices," Proceedings of the 1997 Particle Accelerator Conference (Cat. No.97CH36167), Vancouver, BC, Canada, 1997, pp. 3509-3511 vol.3. doi: 10.1109/PAC.1997.753258.

[10] https://www.esrf.fr/UsersAndScience/Publications/Highlights/2010/axs/axs04